Available online at www.sciencedirect.com

SciVerse ScienceDirect

Ceramics International 38 (2012) 4373–4377

CERAMICS INTERNATIONAL

www.elsevier.com/locate/ceramint

Short communication

Microstructure, mechanical and dielectric properties of highly porous silicon nitride ceramics produced by a new water-based freeze casting

Rubing Zhang *, Daining Fang, Yongmao Pei, Licheng Zhou

State Key Lab. for Turbulence and Complex Systems (LTCS), College of Engineering, Peking University, Beijing 100871, PR China

Received 17 December 2011; received in revised form 2 January 2012; accepted 4 January 2012
Available online 12 January 2012

Abstract

Novel graded porous Si_3N_4 ceramics with different solid content have been fabricated by a new water-based freeze-casting method. A 25 μm-thick surface dense layer on the porous layer was successfully formed without any noticeable defects. A great number of fibrous grains protruding from the internal walls of the macroscopic aligned channels were observed in the porous Si_3N_4 samples with 20–25 vol.% solid content, but little fibrous grains were formed in the sample with 15 vol.% solid content at the similar processing route. As the solid content increasing from 15 to 25 vol.%, the porosity decreased from 76.8% to 66.4%, while the flexural strength and dielectric constants at 10 GHz increased from 14.3 MPa to 33.5 MPa and 1.78 to 2.64, respectively. The dense/porous Si_3N_4 ceramic is feasible in broadband radomes application at high temperature due to ultra-low dielectric constants and moderate strength.

Keywords: A. Sintering; C. Dielectric properties; D. Si_3N_4; E. Functional applications

1. Introduction

Silicon nitride (Si_3N_4) ceramic possesses excellent mechanical properties at both room and elevated temperatures, good thermal shock resistance and excellent ablation resistance, which make it suitable for various promising applications at high temperatures [1–7], but a relatively higher dielectric constant (5.6–5.8 for reactive sintered Si_3N_4 and 7.9–8.2 for hot-pressed Si_3N_4 at 8–10 GHz) limits its applications as a high temperature radomes material [8,9]. Increasing the porosity is an effective way to lower the dielectric constant and loss of Si_3N_4 ceramic, an effect that is particularly remarkable when the porosity is enhanced to 35% or above [10]. Porous Si_3N_4 ceramics can be prepared in different ways, such as, adding fugitive substance [11], gel casting [12], carbothermal nitridation [13], combustion synthesis [14], in situ reaction bonding [15], etc. For example, porous Si_3N_4 ceramics with porosity of 19.4–42.6% were fabricated by the oxidation bonding process, which attained a high flexural strength of 43–137 MPa, a low dielectric constant of 3.1–4.6 and a low dielectric loss of (2.9–4.3) $\times 10^{-3}$ at 1 GHz [15]. Porous Si_3N_4/(Si_3N_4 + BN) sandwich ceramics fabricated by tape casting and hot pressing attained moderate flexural strength of 53.4 MPa, a low dielectric constant of 3.48 (at 1 GHz) [16]. However, the high porosity lowers resistances to moisture and mechanical erosion of porous Si_3N_4 ceramic, so it is necessary to fabricate porous Si_3N_4 ceramic with a dense surface.

Recently, freeze casting as a novel technology has been included during the fabrication of dense/porous layered ceramics [17–20]. For example, Koh et al. [17] obtained a dense/porous layered ceramic by a camphene-based freeze casting. In this process, it is also noted that unidirectional solidification of aqueous slurry may trigger a solid–liquid interface to move rapidly in the initial freezing process, which engulfs the particles in ice to form a dense layer at the bottom of the sample after sintering. Up to now, some important works of the dense/porous ceramics are also produced by freeze casting. Macchetta et al. [18] used camphene-based freeze-casting to fabricate HA/TCP ceramic scaffolds with aligned, interconnected and graded porosity, and the initial solid loading played an important role in the resulting porosity of the scaffolds. Sofie [19] prepared functionally graded and aligned porosity in thin ceramics substrates using TBA-based slurries by freeze-tape casting. The effects of solids loading, freezing temperatures,

* Corresponding author. Tel.: +86 01062757417; fax: +86 01062757417.
E-mail address: rbzhang@pku.edu.cn (R. Zhang).

0272-8842/$36.00
doi:10.1016/j.ceramint.2012.01.012

and solvent type on pore structure were investigated. Zhang et al. [20] fabricated dense/porous bi-layered Al_2O_3 ceramics by introducing an electric field into the freeze-casting process. It was shown that the thickness of the dense layer in the sample could be controlled by tuning the electric field intensity from 51 to 155 μm as the electric field increased from 15 to 90 V.

As above, the final microstructures and properties of the dense/porous ceramics produced by freeze casting depend on the slurry concentration, freezing rate and sintering conditions [21,22]. Moreover, it was found that the water-based freeze-casting method could be used to freeze very dilute ceramic slurries with low solid loading, which, accordingly, allowed ultra-high porosity ceramics with completely interconnected pore channels to be produced. However, till now, the reports on the dielectric properties of dense/porous silicon nitride ceramics fabricated by freeze casting are very scarce. It is difficult to maintain porous Si_3N_4 ceramics with ultra-low dielectric constant (<2.5) and moderate strength. The purpose of the present work is to fabricate dense/porous Si_3N_4 ceramics with ultra-low dielectric constant and moderate strength by a new water-based freeze-casting process. The influence of solid content on the microstructure, mechanical and dielectric properties of porous Si_3N_4 ceramics was also investigated.

2. Experimental procedures

Slurries were prepared by mixing distilled water with 0.3 wt.% ammonium polymethacrylate anionic dispersant (Sigma–Aldrich Trading Co., Ltd., Shanghai, China), glycerol (10 wt.% of solvent), 5 wt.% Y_2O_3 (Sinopharm Chemical Reagent Co., Ltd., Shanghai, China), 3 wt.% Al_2O_3 (Sinopharm Chemical Reagent Co., Ltd., Shanghai, China) and Si_3N_4 (Junyu Ceramic Co., Ltd., Shanghai, China). Slurries were ball-milled with alumina balls for 12 h and de-aired by stirring in a vacuum desiccator. The Si_3N_4 powder consisted of 95 wt.% α-Si_3N_4 and 5 wt.% β-Si_3N_4, and had a mean diameter of 1.5–2.0 μm. The solid loading of the slurries were fixed to 15, 20 and 25 vol.%. The resultant slurries were then poured into graphite molds (Φ50 mm × 10 mm) using a brass bottom plate placed in the cold trap of in a freeze drier (Labconco 77540, Western Medics). The top of the container was open so that the upper surface of the slurry would expose to the cold-air atmosphere at −50 °C, which is higher than the cold trap temperature (−70 °C). Immediately after casting, the ice crystals grow unidirectionally from the surface to the inner of the slurry. Under the previous cooling methods, the freezing-casting techniques could only fabricate the dense/porous bi-layered Si_3N_4 composites by inducing unidirectional solidification of the slurry. In this paper, freezing occurred from surface to the inner of the samples by the new cooling method. The porous layer could be enclosed with the dense layers by inducing multi-directional solidification of the slurry. After freezing, the frozen cast was carefully removed from the mold and the frozen samples were completely freeze-dried under vacuum for 48 h. The green compacts were carefully placed into a graphite crucible with a silicon nitride-based powder bed and sintered in a graphite resistance furnace at 1800 °C for 60 min under a 0.05 MPa nitrogen atmosphere. Both the heating and the cooling rates were 5 °C/min.

The as-prepared products were coated with a thin layer of gold and characterized in a scanning electron microscope (FEI Quanta 200, FEI Company, Hillsboro, USA). The apparent density and porosity of sintered bodies were measured using the Archimedes method. Samples of 3 mm × 4 mm × 35 mm were cut off from the as-sintered porous ceramics, and were loaded at a testing machine (Instron 5569, Instron corp., Canton, USA) to test the flexural strength, with a crosshead speed of 0.05 mm/min. All flexural bars were machined with the tensile surface perpendicular to the freezing direction. In order to obtain the average value, more than six samples of each measurement were chosen. The dielectric properties test is based on measurements of the reflection and transmission moduli between 8.2 and 12.4 GHz, in the fundamental waveguide mode, using standard samples (22.86 mm × 10.16 mm × 3 mm for 8.2–12.4 GHz, Agilent E8326B PNA series network analyzer, USA).

3. Results and discussion

3.1. Microstructure of porous Si_3N_4

Freeze casting of Si_3N_4/water slurry was employed to produce porous Si_3N_4 ceramics with graded and porous structure using different solid content. Fig. 1 shows the schematical illustration of freeze casting system and pore structure formation during freezing casting. These pores were generated by the sublimation of the ice and were aligned along the macroscopic direction of ice formation. During freeze casting, water gradually crystallized to form unidirectionally aligned channel, dendritic pore structure parallel to the freezing direction, running from low temperature of the surface to high temperature of the inner. Meanwhile, the ceramic particles were repelled by the growing ice crystal to cohere together and form strong dense layer. Table 1 shows the variations of porosity, bulk density and linear shrinkage of porous Si_3N_4 ceramics with different solid loading after being sintered at 1800 °C for 60 min. As the solid loading increasing from 15 to 25 vol.%, the bulk density increased from 0.89 to 0.95 g/cm^3, while the porosity and linear shrinkage decreased from 74% to 62% and 25% to 12.6%, respectively. However, the closed porosity increases from 36% to 54% on the contrary because of the blocking effect of the dense layer. Theoretically, if the dense

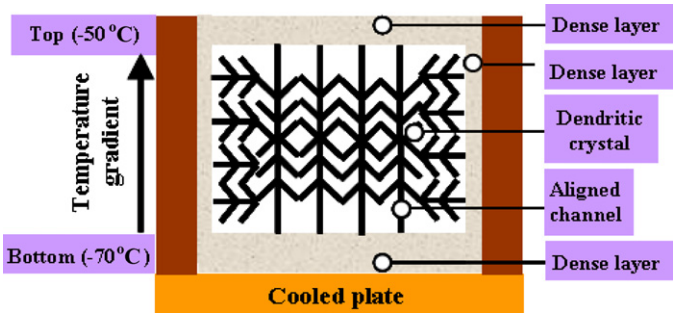

Fig. 1. Schematical illustration of freeze casting system and pore structure formation during freeze casting.

Table 1
Linear shrinkage, total porosity, flexural strength and dielectric constants of the Si_3N_4 porous ceramics with different solid loading.

Solid loading (vol.%)	Linear shrinkage (%)	Porosity (%)		Flexural strength (MPa)	Dielectric constants (8.2–12.4 GHz)
		Total	Closed		
25	12.6	62	54	33.5 ± 4.0	2.46–2.71
20	18.8	66	52	26.9 ± 3.3	1.96–2.11
15	25.0	74	36	14.3 ± 3.6	1.66–1.83

layer on the surface of porous Si_3N_4 ceramic is fully dense, there should be no open pores but closed pores only in specimens. The present tiny holes or defects in the dense layer were generated by the sublimation of the retained ice, and will decrease the closed porosity noticeably because the pores in porous Si_3N_4 ceramic connect well with each other.

Fig. 2(a)–(c) shows the typical microstructure of the porous Si_3N_4 obtained by water-based freeze-casting. Fig. 2(b) shows a top view of the sample, which is the plane parallel to the macroscopic direction of ice formation. It can be seen there is in situ formation of a dense/porous bi-layered Si_3N_4 ceramic. A 25 μm-thick surface dense layer on the porous layer was

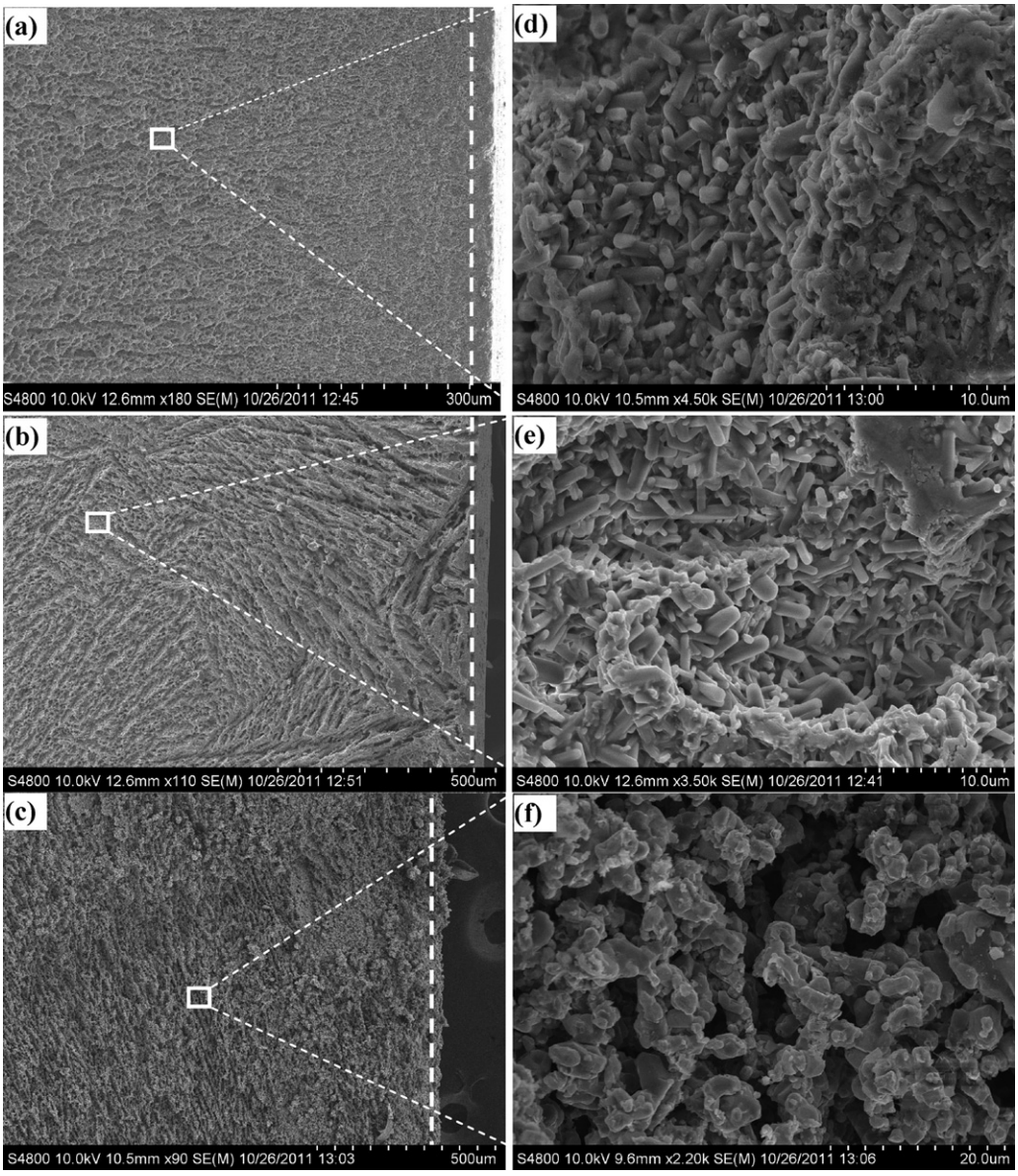

Fig. 2. SEM micrographs of cross section (a–c) and the corresponding details of pore morphology of (d–f) of porous Si_3N_4 ceramics with different solid loading: (a, d) 25 vol.%, (b, e) 20 vol.%, (c, f) 15 vol.%.

successfully formed after sintering at 1800 °C for 60 min without any noticeable defects. Fig. 2(b) suggests that the initial planar ice front is trapping the particles, resulting in a dense layer at the surface of the sample. Afterwards, the formation of a cellular porous microstructure forms, indicating that the columnar ice front is rejecting the particles. This will suggest that initial freezing (the initial 25 μm) is very fast and the ice engulfs the particles. When the ice front velocity decreases, the rejected particles locally pin the ice front, triggering the transition from planar to columnar. A similar phenomenon is also observed by Hong et al. in porous Al_2O_3 ceramics produced by camphene-based freeze-casting [23]. The thickness of the ice crystals is only strongly dependent on the speed of the solidification front. Faster freezing velocities result in larger supercooling in front of the growing crystals that will influence the dense layer thickness. So the dense layer maintained identical thickness at the same freezing conditions in this study whether or not the initial solid content increased or reduced.

As shown in Fig. 2(b), the open pores aligned along the macroscopic direction of ice formation like a channel. Parallel lines trace the dendrite structure generated by the nucleation and growth of the ice in the freezing process. Fig. 2(d)–(f) shows the details of pore morphology and interconnection of grains in the porous Si_3N_4 samples after sintering at 1800 °C with the solid loading varying from 15 to 25 vol.%. It was noted that the microstructures of porous Si_3N_4 ceramics were significantly influenced by the initial solid loading. As the main influencing factor, slurry solid loading determines the microstructure, porosity, and mechanical properties of the final products after sintering at a given temperature. A great number of fibrous grains protruding from the internal walls of the macroscopic aligned channels were observed in the porous Si_3N_4 samples with the solid loading varying from 20 to 25 vol.% (Fig. 2(d)–(e)). However, when the solid loading decreased to 15 vol.%, the Si_3N_4 grains are maintained almost the same particle size of the raw α-Si_3N_4 powder (Fig. 2(f)). Moreover, the typical connection of grains is similar to stone arch bridges and the sintering neck can be easily observed. The samples had homogeneous pore distribution and 3D connection structure with pore size around several microns. It has not been reported for porous Si_3N_4 ceramics in the previous studies. Tatsuki Ohji et al. [3] indicated that the fibrous texture formed through a vapor–solid transformation on the surface was enhanced by the liquid phase. In our work, it is most likely that the liquid glassy phase (SiO_2–Y_2O_3–Al_2O_3) decomposed at elevated temperatures to produce SiO gas. The SiO gas would continuously condense on the surface of the Si_3N_4 grain in the internal wall of the aligned pore, resulting in the growth of the fibrous Si_3N_4 texture [24,25]. As is mentioned above, the lower solid loading results in higher porosity and pore size. When the solid loading decreased to 15 vol.%, the SiO gas would not continuously condense on the surface of the Si_3N_4 grain in the direction of the aligned pore, it may be the reason that little fibrous grains was observed in the sample.

3.2. Mechanical and dielectric properties of porous Si_3N_4 ceramics

The flexural strength of the porous Si_3N_4 ceramics is shown in Table 1. It reveals that the mechanical properties of obtained porous Si_3N_4 ceramics are strongly affected by the microstructure, including pore structure and the morphology of Si_3N_4 grains. Lamellar pores with dendrites in the sample are easy to cause the damage of the obtained porous ceramics. Elongated β-Si_3N_4 grains and suitable interfacial bonding strength would improve the mechanical properties of the samples. As shown in Table 1, the sample with 15 vol.% solid content shows the lowest flexural strength because it has the highest porosity, the biggest pore size and little elongated β-Si_3N_4 grains in the microstructure. As is well-known, the bending strength increases with decreasing porosity. For the samples with 20 vol.% and 25 vol.% solid content, both β-Si_3N_4 content and the aspect ratio of β-Si_3N_4 grains are much higher than that of the sample with 15 vol.% solid content. The bending strength is dominated by both the elongated β-Si_3N_4 grain growth and the densification, and as a result the porosity decreases and the bending strength increases. As the solid loading increasing from 15 to 25 vol.%, the flexural strength increased from 14.3 MPa to 33.5 MPa. Moreover, as shown in Fig. 2(d)–(f), the main lamellar channels in the porous ceramics are interconnected by the dendritic pores, so the rupture might occur along dendritic pores and decrease the mechanical properties. The sample with 25 vol.% solid content exhibits the highest strength in the resultant porous materials. It is attributed to its columnar pore structure with least dendritic pores and highest aspect ratio of β-Si_3N_4 grains.

Dielectric constants of porous Si_3N_4 with different solid content sintered at 1800 °C for 60 min are measured in the frequency range of 8.2–12.4 GHz and the corresponding profiles are presented in Fig. 3. As can be seen from this figure, all the materials exhibited reasonably stable and ultra-low dielectric constant values. It is known that the overall

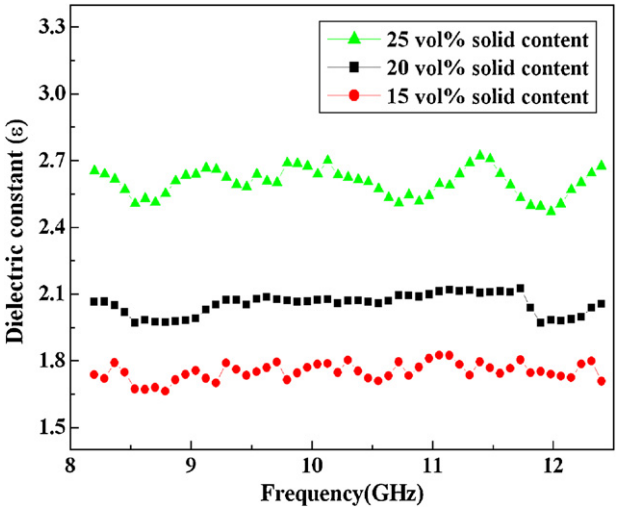

Fig. 3. Dielectric constants of porous Si_3N_4 with different solid content in the frequency range of 8.2–12.4 GHz.

dielectric constant of a material is highly influenced by the material composition, frequency of applied field, temperature of the dielectric, crystal structure, and other external factors including porosity. The processing route is similar in this study, so the observed difference in the dielectric constant data could be related to the change in the porosity. For example, materials with 15 vol.%, 20 vol.% and 25 vol.% solid content have apparent porosities 74%, 66% and 62%, respectively, whereas their corresponding dielectric constant values at 10 GHz are 1.78, 2.07 and 2.64, respectively. So, porosity is the dominating factor for the dielectric constant of porous ceramics in this study, the increase in porosity result in the decrease in dielectric constants. Such low dielectric constants and moderate strength of the dense/porous Si_3N_4 ceramic will draw much attention for potential dielectric applications at high temperature.

4. Conclusions

Highly porous Si_3N_4 ceramics with graded and porous structures have been fabricated by a new water-based freeze-casting method. The typical pore structure includes surface dense layer, aligned channel and dendritic pore using cold-air as cooled agent. The influence of solid content on the microstructure, mechanical and dielectric properties of porous silicon nitride ceramics was studied in this paper, the following results were obtained.

(1) In this study, whether or not the initial solid content increased or reduced, a 25 μm-thick surface dense layer on the porous layer was successfully formed after sintering at 1800 °C for 60 min without any noticeable defects. A great number of fibrous grains protruding from the internal walls of the macroscopic aligned channels were observed in the porous Si_3N_4 samples with 20 vol.% and 25 vol.% solid content, however, little fibrous grains were formed in the sample with 15 vol.% solid content.
(2) As the solid content increasing from 15 to 25 vol.%, the porosity decreased from 76.8% to 66.4%, while the flexural strength and dielectric constants at 10 GHz increased from 14.3 MPa to 33.5 MPa and 1.78 to 2.64, respectively. The ultra-low dielectric constants and moderate strength of the dense/porous Si_3N_4 ceramic will draw much attention for the broadband radome application at high temperature.

Acknowledgements

This work was supported by the National Natural Science Foundation of China (91016021 and 11102003) and China Postdoctoral Science Foundation Funded Project (20110490196).

References

[1] F.L. Riley, Silicon nitride and related materials, J. Am. Ceram. Soc. 83 (2) (2000) 245–265.
[2] Y. Inagaki, O.T. Kondon, High performance porous silicon nitrides, J. Eur. Ceram. Soc. 22 (2002) 2489–2494.
[3] J.H. She, J.F. Yang, D.D. Jayaseelan, N. Kondo, T. Ohji, S. Kanzaki, Y. Inagaki, Thermal shock behavior of isotropic and anisotropic porous silicon nitride, J. Am. Ceram. Soc. 86 (2003) 738–740.
[4] D.S. Fox, E.J. Opila, Q.N. Nguyen, D.L. Humphrey, S.M. Lewton, Para-linear oxidation of silicon nitride in a water-vapor/oxygen environment, J. Am. Ceram. Soc. 86 (2003) 1256–1261.
[5] R.M. Backhaus, V. Guerin, A.M. Huntz, V.S. Urbanovich, High temperature oxidation behavior of high-purity alpha- beta-, and mixed silicon nitride ceramics,, J. Am. Ceram. Soc. 85 (2002) 385–392.
[6] Y. Zhang, Y.B. Cheng, S. Lathabai, K. Hirao, Erosion response of highly anisotropic silicon nitride, J. Am. Ceram. Soc. 88 (2005) 114–120.
[7] A. Zerr, M. Kempf, M. Schwarz, E. Kroke, M. Goken, R. Riedel, Elastic moduli and hardness of cubic silicon nitride, J. Am. Ceram. Soc. 85 (2002) 86–90.
[8] J.D. Walton, Reaction sintered silicon nitride, in: Proceedings of the 11th Symposium on Electromagnetic Windows, Georgia Institute of Technology, Atlanta, GA, 1972.
[9] J. Barta, M. Manela, R. Fischer, Si_3N_4 and Si_2N_2O for high performance radomes, Mater. Sci. Eng. A 71 (1984) 265–272.
[10] X.M. Li, X.W. Yin, L.T. Zhang, L.F. Cheng, Y.C. Qi, Mechanical and dielectric properties of porous Si_3N_4–SiO_2 composite ceramics, Mater. Sci. Eng. A 500 (2009) 63–69.
[11] D. Aranzazu, H. Stuart, Characterisation of porous silicon nitride materials produced with starch, J. Eur. Ceram. Soc. 24 (2) (2004) 413–419.
[12] J.L. Yu, H.J. Wang, J. Zhang, Neural network modeling and analysis of gel casting preparation of porous Si_3N_4 ceramics, Ceram. Int. 35 (2009) 2943–2950.
[13] S.Y. Shan, J.F. Yang, J.Q. Gao, W.H. Zhang, Z.H. Jin, Porous silicon nitride ceramics prepared by reduction-nitridation of silica, J. Am. Ceram. Soc. 88 (9) (2005) 2594–2596.
[14] D.Y. Chen, B.L. Zhang, H.R. Zhuang, W.L. Li, Combustion synthesis of network silicon nitride porous ceramics, Ceram. Int. 29 (4) (2003) 363–364.
[15] S.Q. Ding, Y.P. Zeng, D.L. Jiang, Oxidation bonding of porous silicon nitride ceramics with high strength and low dielectric constant, Mater. Lett. 61 (2007) 2277–2280.
[16] K.H. Zuo, Y.P. Zeng, D.L. Jiang, The mechanical and dielectric properties of Si_3N_4-based sandwich ceramics, Mater. Des. 35 (2012) 770–773.
[17] Y.H. Koh, I.K. Jun, J.J. Sun, H.E. Kim, In situ fabrication of a dense/porous bi-layered ceramic composite using freeze casting of a ceramic-camphene slurry, J. Am. Ceram. Soc. 89 (2) (2006) 763–766.
[18] A. Macchetta, I.G. Turner, B.C. Rowen, Fabrication of HA/TCP scaffolds with a graded and porous structure using a camphene-based freeze-casting method, Acta Biomaterialia 5 (2009) 1319–1327.
[19] S.W. Sofie, Fabrication of functionally graded and aligned porosity in thin ceramic substrates with the novel freeze-tape-casting process, J. Am. Ceram. Soc. 90 (2007) 2024–2031.
[20] Y.M. Zhang, L.Y. Hu, J.C. Han, Preparation of a dense/porous bi-layered ceramic by applying an electric field during freeze casting, J. Am. Ceram. Soc. 92 (8) (2009) 1874–1876.
[21] S. Deville, E. Saiz, A.P. Tomsia, Freeze casting of hydroxyapatite scaffolds for bone tissue engineering, Biomaterials 27 (32) (2006) 5480–5489.
[22] S. Deville, E. Saiz, A.P. Tomsia, Ice-templated porous alumina structures, Acta Mater. 55 (6) (2007) 1965–1974.
[23] C.Q. Hong, J.C. Du, J. Liang, X.H. Zhang, J.C. Han, Functionally graded porous ceramics with dense surface layer produced by freeze-casting, Ceram. Int. 37 (2011) 3717–3722.
[24] K. Yokoyama, S. Wada, Solid–gas reaction during sintering of Si_3N_4 ceramics, J. Ceram. Soc. Jpn. 108 (1) (2000) 6–9.
[25] C. Kawai, A. Yamakawa, Coating of fine-grained Si_3N_4 whiskers on a porous Si_3N_4 substrate by gas phase processing for membrane filter application, J. Ceram. Soc. Jpn. 107 (10) (1999) 961–967 (in Japanese).